Nanofluid and Micropolar Fluid Flow over a Shrinking Sheet with Heat Transfer

[1]Srinivas Maripala, [2]Kishan.N,
[1]*Department of Mathematics, SNIST, Ghatkesar,Telangana, India, 501301.*
[2]*Department of Mathematics, OU, Telangana, India, 500007.*

Abstract:
This analysis investigated with the boundary layer flow and heat transfer aspects of a micropoloar nanofluid over a porous shrinking sheet with thermal radiation. The boundary layer equations governed by the partial differential equations are transformed in to a set of ordinary differential equations with the help of suitable local similarity transformations. The coupled nonlinear ordinary differential equations are solved by the implicit finite difference method along with the Thamous algorithm. Dual solutions of dimensionless velocity, angular velocity, temperature and concentration profiles are analyzed by the effect of various controlling flow parameters viz., Lewis number Le, thermophoresis Nt, Brownian motion parameter Nb, Radiation parameter R, Prandtl number Pr, material parameter K, mass suction parameter S, magnetic parameter M. Physical quantities such as skin frication coefficient, local heat, local mass fluxes are also computed and are shown in a table.

Keywords: *MHD, micropolar fluid flow, thermal radiation, nanofluid, shrinking sheet.*

1. Introduction: In last few decades, the research interest in micropolar fluid theory has significantly increased due to its enormous applications in many industrial processes. A micropolar fluid is the fluid with internal structures in which coupling between the spin of each particle and the macroscopic velocity field is taken into account. It is a hydro dynamical framework suitable for angular systems which consist of particles with macroscopic size. Unlike the other fluids, micropolar fluids may be described as non-Newtonian fluids consisting of dumb-bell molecules or short rigid cylindrical element, polymer fluids, fluid suspension, etc. In addition with the classical velocity field, a microrotation vector and a gyration parameter are introduced in the micropolar fluid model in order to investigate the kinematics of microrotation. The theory of micropolar fluids, first proposed by Eringen [1,2] can be used to study the behaviors of exotic lubricants, polymeric suspensions, muddy and biological fluids, animal blood, colloidal solutions, liquid crystals with rigid molecules, etc. The presence of dust or smoke, in particular in a gas may also be modeled using micropolar fluid dynamics. Analysis of the flow and heat transfer of micropolar fluid in a vertical channel has been of great interest because the Navier–Stokes equations for Newtonian fluids cannot successfully describe the characteristics of fluid with suspended particles. Comprehensive reviews of the theory and applications can be found in the review articles by Ariman et al. [3, 4] and the recent books by Lukaszewicz [5] and Eringen [6]. The pioneering work of Eringen [1] was extended in boundary layer theory by Peddieson and McNitt [7]. Peddieson [8] applied the micropolar fluid model in turbulent flow also. The self-similar solution of boundary layer flow of a micropolar fluid over a semi-infinite flat plate was obtained by Ahmadi [9]. Kummerer [10] studied the steady two-dimensional flow of micropolar fluid using a numerical technique. BS Malga and Kishan.N [11] studied the unsteady free convection and mass transfer boundary layer flow past an accelerated infinite vertical porous plate with suction by taking into account the viscous dissipation is considered when the plate accelerates in its own plane. Guram and Smith [12] investigated the stagnation point flow of a micropolar fluid in an infinite plate with two different boundary conditions – vanishing spin and vanishing spin gradient. The free convective boundary layer flow of a thermomicropolar fluid over a non-isothermal vertical flat plate was discussed by Jena and Mathur [13]. Gorla [14] studied the micropolar boundary layer flow near a stagnation point on a moving wall.

In a continuation study of flow over a stretching sheet, considerable interest has been placed on fluid flow over a shrinking sheet. The study of viscous flow over a shrinking sheet with suction effect at the boundary was first investigated by Miklavcic and Wang [15]. Following this pioneering work, many papers on this topic have been published. For such problem, the movement of the sheet is in the opposite direction to that of the stretching case, and thus the flow moves towards a slot. Goldstein [16] has described the shrinking flow which is basically a backward flow. The existence and uniqueness of steady viscous flow due to a shrinking sheet was established by Miklavcic and Wang [17] considering the suction effects and they concluded that for some specific values of suction, dual solutions exist and also in certain range of suction, no boundary layer solution is possible. The boundary layer flow

near a shrinking sheet is given significant attention due to its increasing engineering applications. The flow development around the shrinking sheet was demonstrated by Wang [18] while studying behavior of liquid film on an unsteady stretching sheet. Fang [19] studied the boundary layer flow over a continuously shrinking sheet with power-law surface velocity and with mass transfer. Fang and Zhang [20] obtained a closed-form analytical solution for MHD viscous flow over a shrinking sheet subjected to applied suction through the porous sheet. The unsteady viscous flow over a continuously shrinking sheet with mass suction was investigated by Fang et al. [21]. Bhattacharyya [22] investigated the steady boundary layer flow and heat transfer over an exponentially shrinking sheet. Ishak et al. [23] described the boundary layer flow of non-Newtonian power-law fluid past a shrinking sheet with suction and Yacob and Ishak [24] discussed the micropolar fluid flow over a shrinking sheet. Wang's [25] problem was extended by many researchers showing various aspects of shrinking sheet flow. Radiative heat transfer in the boundary layer flow is very important from application point of view, because the quality of the final product is very much dependent on the rate of heat transfer of the ambient fluid particles. Elbashbeshy [26] discussed the effect of radiation on the forced convection flow of along a heated horizontal stretching surface. Bhatacharyya and Layek [27] demonstrated the radiation effects on the steady stagnation-point flow and heat transfer towards a permeable shrinking sheet.

The ''nanofluid'' term was first introduced by Choi [28] to describe the mixture of nanoparticles and base fluid such as water and oil. The addition of nanoparticle into the base fluid is able to change the transport properties; flow and heat transfer capability of the liquids and indirectly increase the low thermal conductivity of the base fluid which is identified as the main obstacle in heat transfer performance. This mixture has attracted the interest of numerous researchers because of its many significant applications such as in the medical applications, transportations, microelectronics, and chemical engineering, aerospace and manufacturing. A comprehensive literature review on nanofluids has been given by Li et al. [29], Kakac and Pramuanjaroenkij [30]. Hunegnaw D and Kishan.N [31] studied the the magnetohydrodynamic boundary layer flow and heat transfer of a nanofluid past a nonlinearly permeable stretching/shrinking sheet with thermal radiation and suction effect in the presence of chemical reaction. Wong and De Leon [32], Saidur et al. [33] and most recently by Mahian et al. [34]. These papers are based on the mathematical nanofluid models proposed by Khanafer [35] and Tiwari and Das [36] for the two-phase mixture containing micro-sized particles. On the other hand, one should also mention the mathematical nanofluid model proposed by Buongiorno [37] used in many papers pioneered by Nield and Kuznetsov [38], and Kuznetsov and Nield [39] for the free convection boundary layer flow along a vertical flat plate embedded in a porous medium or in a viscous fluid. In this model, the Brownian motion and thermophoresis enter to produce their effects directly into the equations expressing the conservation of energy and nanoparticles, so that the temperature and the particle density are coupled in a particular way, and that results in the thermal and concentration buoyancy effects being coupled in the same way.

Srinivas Maripala and Kishan.N,[40], studied the Unsteady MHD flow and heat transfer of nanofluid over a permeable shrinking sheet with thermal radiation and chemical reaction. Recently, Krishnendu Bhattacharyya et.al.[41] studied the Effects of thermal radiation on micropolar fluid flow and heat transfer over a porous shrinking sheet.

The main goal of the present study in to investigate the MHD flow and heat transfer in micropolar nanofluid over a porous shrinking sheet with thermal radiation are studied. It is very interesting to investigate the simultaneous effects of the thermal radiation and the microrotation on the steady flow. The nonlinear self-similar ordinary differential equations obtained here are solved numerically by finite difference technique with the help of Cranck-Nicklson method using Thomus algoritham. The complete effects of several parameters are discussed in detail.

2. Analysis of the flow problem:

Consider, unsteady two-dimensional laminar boundary layer flow of incompressible electrically conducting viscous microploar nanofluid and heat transfer a porous shrinking sheet with thermal radiation. The flow is subjected to a transverse magnetic field of strength B_0, which is assumed to be applied in the positive $y-$ direction, normal to the surface. It is assumed that the velocity of the shrinking sheet $U_W = -C_X$ with c > 0 being shrinking constant. Using boundary layer approximation, the equations of motion for the micropolar nanofluid and heat transfer may be written in usual notation as:

$$\frac{\partial u}{\partial x} + \frac{\partial v}{\partial y} = 0 \qquad (1)$$

$$u\frac{\partial u}{\partial x}+v\frac{\partial u}{\partial y}=\left(v+\frac{k}{\rho}\right)\frac{\partial^2 u}{\partial y^2}+\frac{k}{\rho}\frac{\partial N}{\partial y}-\frac{\sigma B_0^2}{\rho}u \quad (2)$$

$$u\frac{\partial N}{\partial x}+v\frac{\partial N}{\partial y}=\frac{Y}{\rho j}\frac{\partial^2 N}{\partial y^2}-\frac{k}{\rho j}(2N+\frac{\partial u}{\partial y}) \quad (3)$$

$$u\frac{\partial T}{\partial x}+v\frac{\partial T}{\partial y}=\frac{k^*}{\rho C_p}\frac{\partial^2 T}{\partial y^2}-\frac{1}{\rho C_p}\frac{\partial q_r}{\partial y}-\tau[D_B\frac{\partial C}{\partial y}\frac{\partial T}{\partial y}+\frac{D_T}{T_\infty}\left(\frac{dT}{dy}\right)^2] \quad (4)$$

$$u\frac{\partial C}{\partial x}+v\frac{\partial C}{\partial y}=D_B\frac{\partial^2 C}{\partial y^2}+\frac{k}{\rho}\frac{\partial N}{\partial y}+\frac{D_T}{T_\infty}(\frac{dT}{dy})^2 \quad (5)$$

Subject to the boundary conditions:

$$u=U_w=-cx\,,=v_w\,,N=-m\frac{\partial u}{\partial y}\,,\quad T=T_w\quad C=C_w \text{ at } y=0\,, \quad (6)$$

And $u\longrightarrow 0$, $N\longrightarrow 0$, $T\longrightarrow T_\infty$ and $C\ tends\ to\ C_\infty$ as y tends to ∞,

Where u and v are velocity components in x and y direction respectively, $v(=\mu/\rho)$ is the kinemetic fluid viscosity, ρ is the fluid density, μ is the dynamic viscosity, N is the microrotation or angular velocity whose direction is normal to the xy -plane, j is microinertia per unit mass, γ is spin gradient viscosity, k is the vortex viscosity (gryo-viscosity,) T is the temperature, C is the concentration of the fluid, k^* is the thermal conductivity of the fluid, C_p is the specific heat, q_r is the radiative heat flux, T_w and C_w - the temperature and concentration of the sheet, T_∞ and C_∞- the ambient temperature and concentration, D_B - the Brownian diffusion coefficient, D_T the thermophoresis coefficient, B_0 - the magnetic induction, $(\rho C)_p$ - the heat capacitance of the nanoparticles, $(\rho C)_f$- the heat capacitance of the base fluid, and $\tau=(\rho C)_p/(\rho C)_f$ is the ratio between the effective heat capacity of the nanoparticles material and heat capacity of the fluid. Here, v_w is the wall mass transfer velocity with $v_w<0$ for mass suction and $v_w>0$ for mass injection. We note that m is constant such that 0≤m≤1. The case m=0 indicates $N=0$ at the surface. It presents flow of concentrated particle in which the microelements closed to the wall surface are unable to rotate [42]. This case is also known as strong concentration of microelements [43]. The case m=0.5 indicates the vanishing of the anti-symmetric part of the stress tensor and denotes weak concentration of microelements [44]. Whereas, the case m=1 suggested by Peddiesion [45] is used for the modeling of turbulent boundary layer flows. Following, Ahmadi [44], Gorla [46], or Ishak et al. [47], we assumed that spin gradient viscosity y is given by :

$$\gamma=(\mu+k/2)j\ =(\mu(1+k/2)j\,, \quad (7)$$

where $K=k/\mu$ is the material parameter. This assumption is in voked o allow the field of equations to predict the correct behavior in the limiting case when the microstructure effects become negligible and the total spin N reduces to the angular velocity[44].

Using Rosseland's approximation for radiation [48], we obtain $q_r=-(4\sigma/3k_1)\,\partial T^4/\partial y$ where σ the Stefan-Boltzman constant is, k_1 is the absorpation coefficient. We presume that the temperature variation within the flow is such that T^4 may be expanded in a Taylor's series. Expanding T^4 about T_∞ and neglecting higher order terms we get, $T^4=4\,T_\infty^3\,T-3\,T_\infty^4$

Now Eq.(4) reduces to:

$$u\frac{\partial T}{\partial x}+v\frac{\partial T}{\partial y}=\frac{k^*}{\rho C_p}\frac{\partial^2 T}{\partial y^2}+\frac{16\sigma T_\infty^3}{3k_1\rho C_p}\frac{\partial^2 T}{\partial y^2}-\tau[D_B\frac{\partial C}{\partial y}\frac{\partial T}{\partial y}+\frac{D_T}{T_\infty}\left(\frac{dT}{dy}\right)^2] \quad (8)$$

The following transformations are introduced :

$$\psi=(cv)^{\frac{1}{2}}\,X\,f(\eta),\quad N=cX(c/v)^{\frac{1}{2}}\,h(\eta)\,,=T_\infty+(T_w-T_\infty)\,\theta(\eta)\,,\quad C=C_\infty+(C_w-C_\infty)\,\varphi(\eta),\quad \eta=(c/v)^{\frac{1}{2}}\,y \quad (9)$$

Where ψ is the stream function defined in the usual notation as $u = \partial\psi/\partial y$ and $v = -\partial\psi/\partial x$ and η is the similarity variable.

Now, Eq. (1) is identically satisfied and the Eqs.(2), (3) and (8) reduce to the following nonlinear self-similar ordinary differential equations :

$$(1+K)f''' + ff'' - f'^2 + Kh' - Mf' = 0 \quad (10)$$

$$(1+K/2)h'' + fh' - f'h - K(2h + f'') = 0 \quad (11)$$

$$(3R+4)\theta'' + 3RPrf\theta' + \Pr(Nb\,\theta' + Nt\,\theta'^2) = 0 \quad (12)$$

$$\varphi'' + Lef\varphi' + \frac{Nt}{Nb}\theta'' = 0 \quad (13)$$

Where primes denote differential with respect to η. M- $Pr = \mu C_p/k^*$ is the Prandtl number , $Nb = \tau D_B(C_w - C_\infty)/v$ is Brownian motion parameter, $Nt = \tau D_T(T_w - T_\infty)/vT_\infty$ is thrmophoresis parameter, $Le = v/D_B$ is Lewis number and $R = k^*K_1/4\sigma T_\infty^3$ is the thermal radiation parameter. The transformed boundary conditions are

$f(\eta) = S, f'(\eta) = -1,\ h(\eta) = -m\,f''(\eta)\ ,\ \theta(\eta) = 1\ ,\varphi(\eta) = 1$ at η = 0

And $f'(\eta) tends\ to\ 0$, $h'(\eta) tends\ to$ 0, $\theta'(\eta) tends\ to$ 0 , $\varphi'(\eta)\ tends\ to\ 0$ as η tends to ∞

And where $S = -v_w/(c\,v)^{\frac{1}{2}}$ is wall mass transfer parameter, S>0 corresponds to mass suction and $S < 0$ corresponds to mass injection.

Table I: Numerical values of $f''(0)$, $g'(0)$,$-\theta'(0)$ *and* $-\phi'(0)$ at the sheet for different values of Nt ,*Nb*,*Le and M* when K=0.1,m=0.5,Pr=1.0,R=1.0.

		$f''(0)$	$g'(0)$	$-\theta'(0)$	$-\phi'(0)$
Nt	0.1	-0.654881	-0.253793	1.085830	2.326034
	0.2	-0.64741	-0.249314	1.065970	2.216199
	0.3	-0.63809	-0.234939	1.066430	2.107338
	0.4	-0.62081	-0.220668	1.069200	1.999418
	0.5	-0.619554	-0.216498	0.998283	1.992407
Nb	0.1	-0.602010	-0.221426	1.111610	1.30727
	0.2	-0.635423	-0.229303	1.065070	1.88328
	0.3	-0.646809	-0.244939	1.026430	2.07338
	0.4	-0.652032	-0.247504	0.990473	2.16771
	0.5	-0.654779	-0.248841	0.956098	2.22387
Le	1	-0.444950	-0.144039	1.27846	-0.185624
	10	-0.649813	-0.236340	1.12596	1.999160
	20	-0.683747	-0.254022	1.10025	3.160030
	50	-0.714107	-0.270606	1.08001	5.353600
	100	-0.729246	-0.279186	1.07134	7.757390
M	0	-0.902584	-0.3743770	0.976165	2.03765
	5	-0.772424	-0.3042750	1.002770	2.05617
	10	-0.646809	-0.2349390	1.026430	2.07338
	20	-0.524913	-0.1662230	1.047850	2.08950
	50	-0.406157	-0.0980246	1.087500	2.10473

3. Results:

The computations have been carried out for various flow parameters such as mass suction parameter S, magnetic parameter M, Lewis number Le, thermophoresis parameter Nt, Brownian motion parameter Nb, radiation parameter R, Prandtl number Pr, material parameter K. The values of skin frication coefficient $f''(0)$, stress coefficient $h'(0)$, Nusselt number coefficient $-\theta'(0)$, Sherwood number coefficient $-\varphi'(0)$ for different values of thermophoresis parameter Nt, Brownian motion parameter Nb, Lewies number Le, magnetic parameter M are calculated and shown in table I. It is evident that with the increase of thermophoresis parameter Nt the skin frication coefficient $f''(0)$ and stress coefficient $h'(0)$ increases and the Nusselt number coefficient $-\theta'(0)$, Sherwood number coefficient $-\varphi'(0)$ decreases with the increase of thermophoresis parameter Nt. The effect of Brownian motion parameter Nb is to decreases the skin frication coefficient $f''(0)$, stress coefficient $h'(0)$ and Nusselt number coefficient $-\theta'(0)$ values, where as it increases Sherwood number coefficient $-\varphi'(0)$ it is evident from the table that the effect of magnetic parameter M is leads to enhance the values of skin frication coefficient $f''(0)$, , stress coefficient $h'(0)$ and Nusselt number $-\theta'(0)$ and the , Sherwood number coefficient $-\varphi'(0)$.

Figure 1(a)-1(d) shows that for both first and second solution for velocity, angular velocity, temperature, and concentration profiles respectively, for different values of mass suction parameter S. For first solution the velocity profiles f' decreases with the increasing in mass suction parameter S, while for second solution the velocity profiles increases with increasing in mass suction parameter S. From figure 1(b) it is noticed that the angular velocity increases with the increasing of mass suction parameter S for both dual solutions. It can be observed from figure 1(c) that the temperature profiles decrease with the increase of mass suction parameter S, where as the temperature profiles increases with the increase of mass suction parameter S for the second solution. It is also noticed that the concentration profiles decreases with the increase of mass suction parameter S for both dual solutions.

Figure 2(a) represents the effect of constant m for velocity profiles. It is observed that the velocity profiles decreases with the increase of m for first solution and increases in the second solution. The angular velocity decreases with the increase of m is observed from figure 2(b). Figure 2(c) depicts that the increasing m leads to decreases the temperature profiles for first solution and increasing the temperature profiles with the increase of m in second solution. Figure 2(d) shows that increasing m enhance the concentration for both first and second solutions. In figure 3(a) the dual velocity profiles shows that the velocity profiles increases with the increase of magnetic parameter M for both these solutions. The effects of magnetic parameter M enhance the dual angular velocity profiles for first and second solutions. In figure 3(c) shows that the dual temperature profiles for several values of magnetic parameter M. As the increasing magnetic parameter M enhance the temperature profiles for first and second solutions. Figure 3(d) depict the dual concentration profiles for the effect of magnetic field parameter M, as the magnetic parameter M increases the concentration profiles decreases for first and second solutions. The variations in velocity, angular, temperature and concentration profiles distribution for several values of thermophoresis parameter Nt respectively. The effect of thermophoresis parameter Nt reduces as increases with the increase of thermophoresis parameter Nt for both solutions. It is observed that an increase of thermophoiresis parameter Nt leads to increased the angular velocity profiles for both first and second solutions is also noticed that an increases the value of Nt results increasing the temperature profiles and concentration profiles for both first and second solutions. Therefore with increase of thermophoresis parameter Nt temperature distribution for both the solutions. The effect of Brownian motion parameter Nb on dual velocity, angular, temperature and concentration profiles are shown in fig 5(a) - 5(d). It is observed from the figure that the effect of Brownian motion parameter Nb reduces the velocity profiles for both first and second solutions. It is also noticed from figure 5(b) the influence of Brownian motion parameter Nb is to enhance the angular velocity for second solution, where as reduce for first solution. The reverse phenomenon is observed for both the solutions for accuracy from the boundary. The influence of Nb on dual temperature increases with the increase of Nb for both the solutions. This is due to enhance molecular activity at higher values of Nb which increase fluid motion and transport of heat energy their diffusion. But the nanoparticle fraction profiles decreases for both the first and second solutions with the increasing of Brownian motion parameter Nb.

The variations in velocity, angular velocity and temperature profiles for different values of material parameter K are demonstrated in figure 6(a)-6(c). From figure 6(a), it is evident that the velocity profiles $f'(\eta)$ values decreases with the increasing of material parameter K for first solution, while, it increases with the material parameter K. In the second solution, the dual angular velocity profiles $h(\eta)$ in figure 6(b) show that the angular velocity values increases as material parameter K decreases for both first and second solution. From the figure 6(c), it is observed

that with the increasing values of material parameter K the thermal boundary layer thickness increases for first solution and it decreases for second solution.

The Lewis Number Le effects on velocity and concentration profiles are explained from the figure 7(a) – 7(b). From figure 7(a), it is claimed that the velocity profiles are decreases with the increasing of Lewis number Le in both first and second solution. The reverse phenomenon observed in figure 7(b) that is the temperature profiles increases with the increase of Lewis number Le. Figure 8 and 9 represents the influence of Prandtl number Pr and the radiation parameter R on the dimensional less temperature profiles. It is observed that the thermal conductivity of the fluid reduces with the increase of Prandtl number Pr increases same phenomenon is noticed for both first and second solutions. The dual temperature profiles are decreases with the increase in radiation parameter R is noticed for both first and second solutions from figure 9.

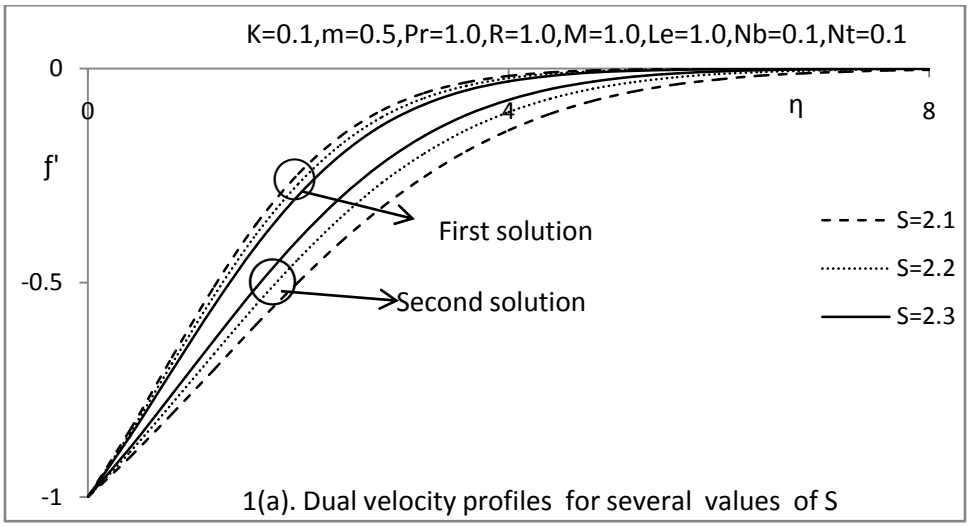

1(a). Dual velocity profiles for several values of S

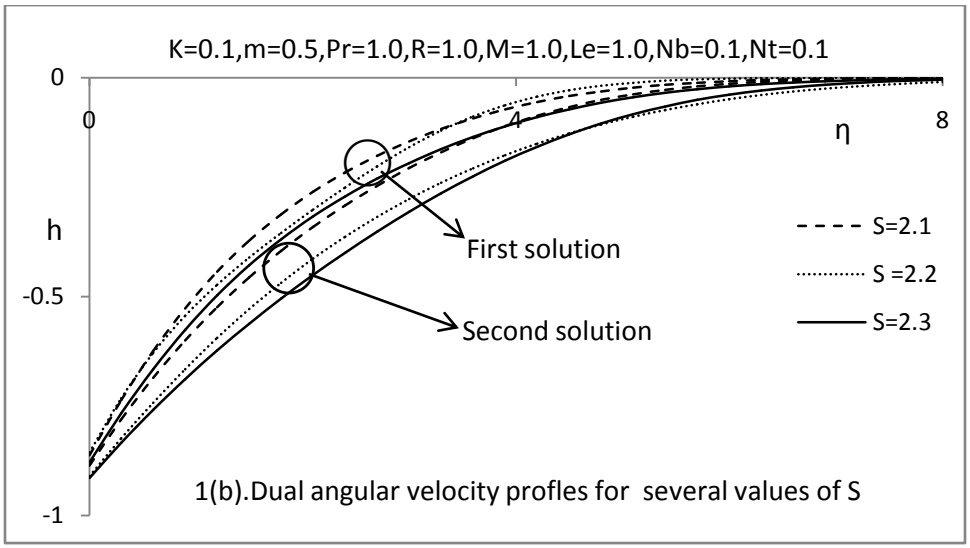

1(b).Dual angular velocity profles for several values of S

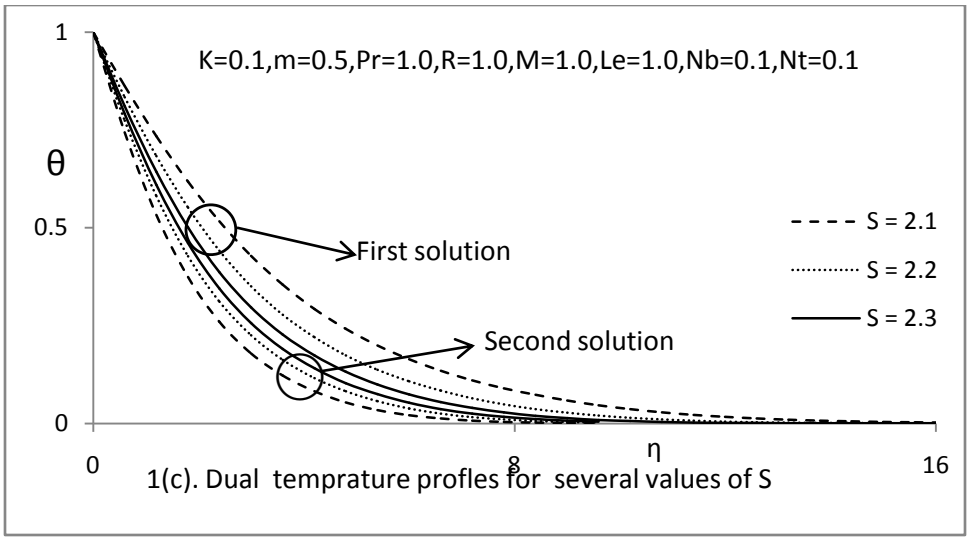

1(c). Dual temprature profles for several values of S

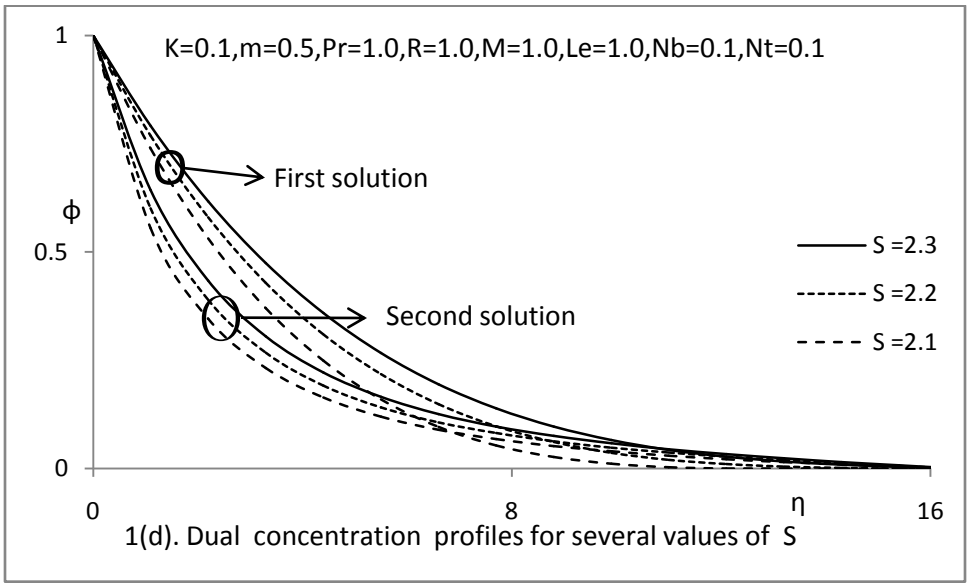

1(d). Dual concentration profiles for several values of S

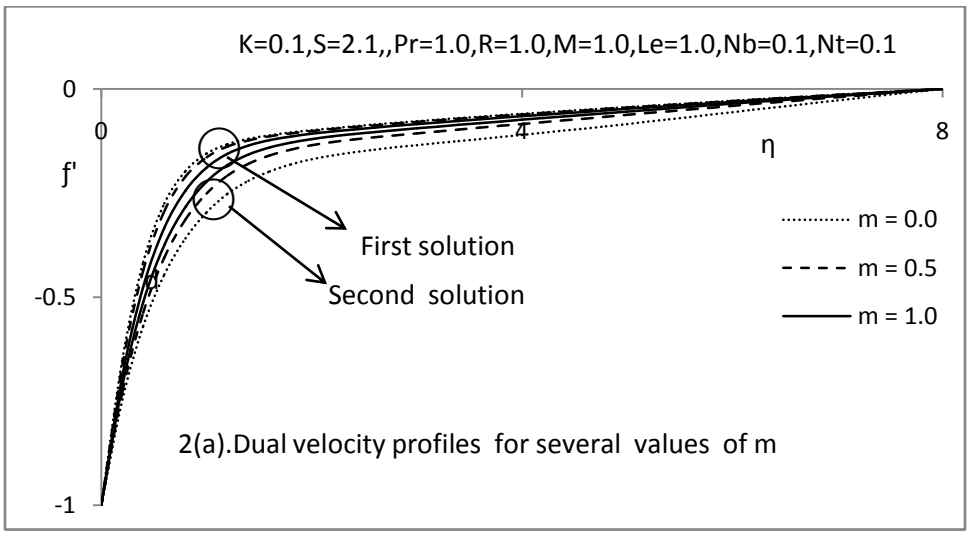

2(a).Dual velocity profiles for several values of m

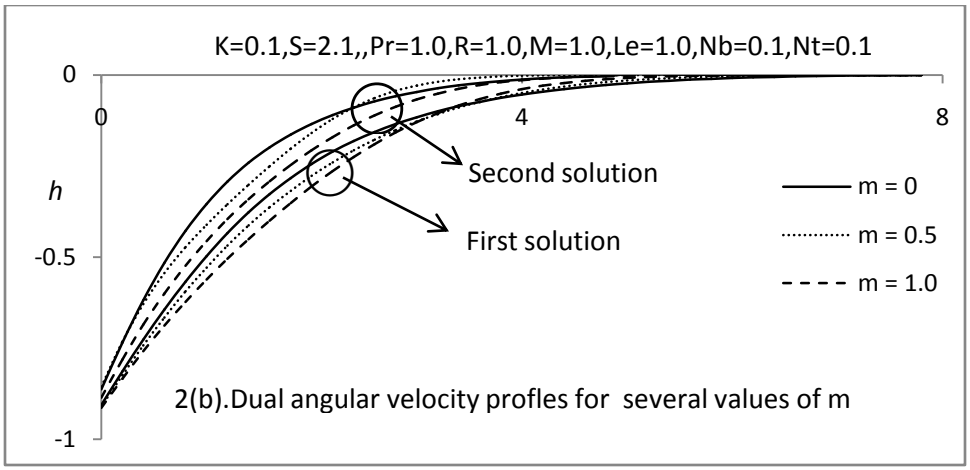

2(b).Dual angular velocity profles for several values of m

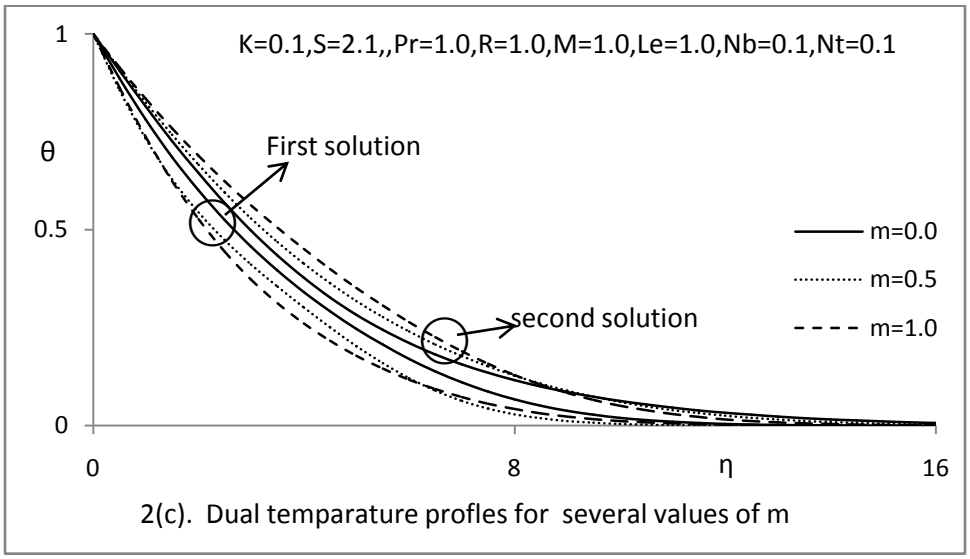

2(c). Dual temparature profles for several values of m

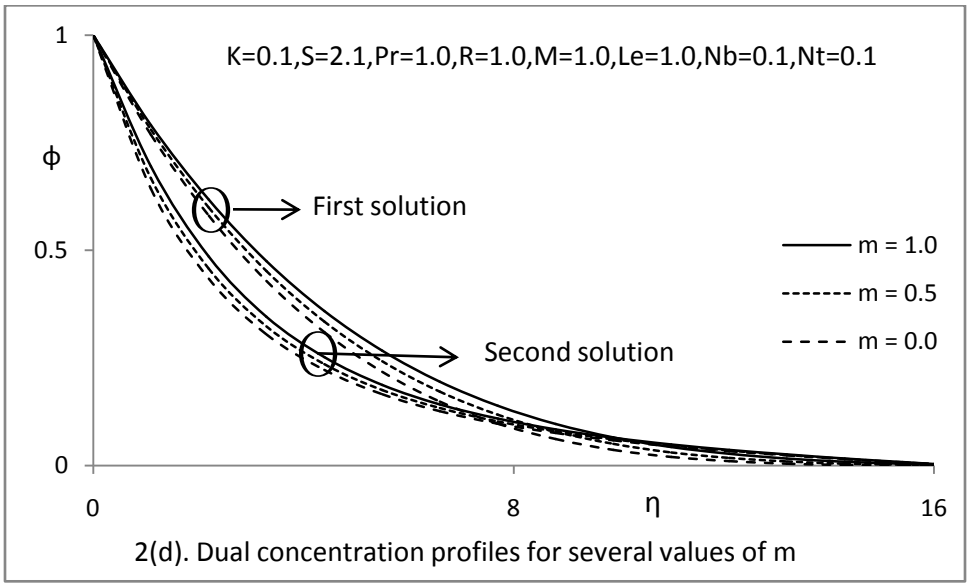

2(d). Dual concentration profiles for several values of m

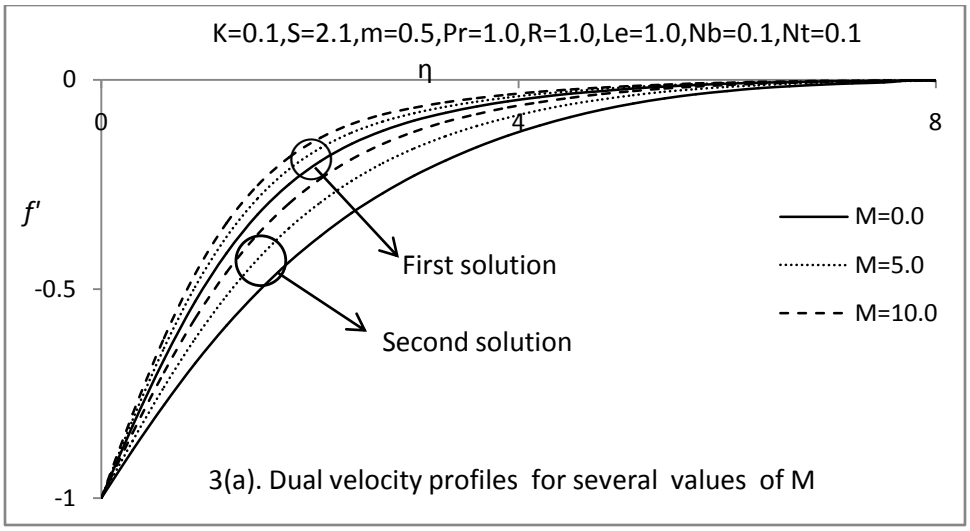

3(a). Dual velocity profiles for several values of M

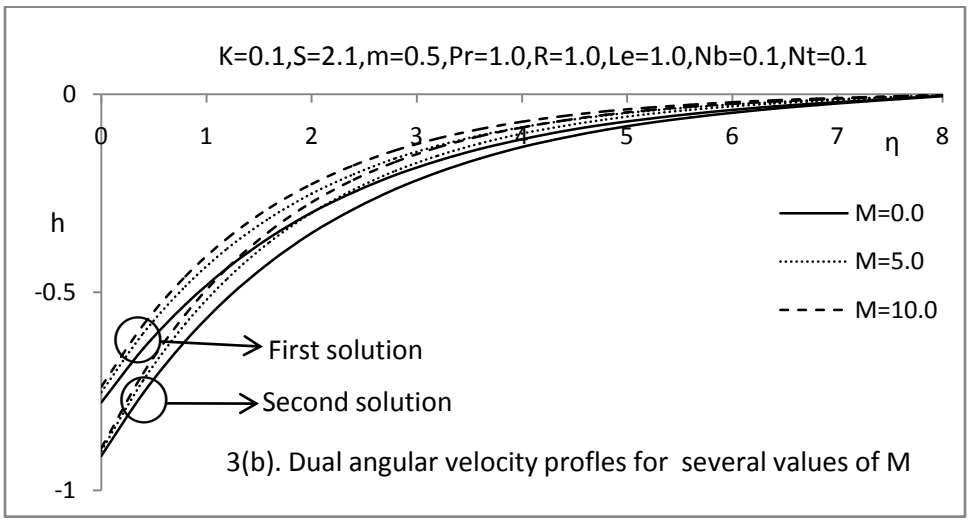

3(b). Dual angular velocity profles for several values of M

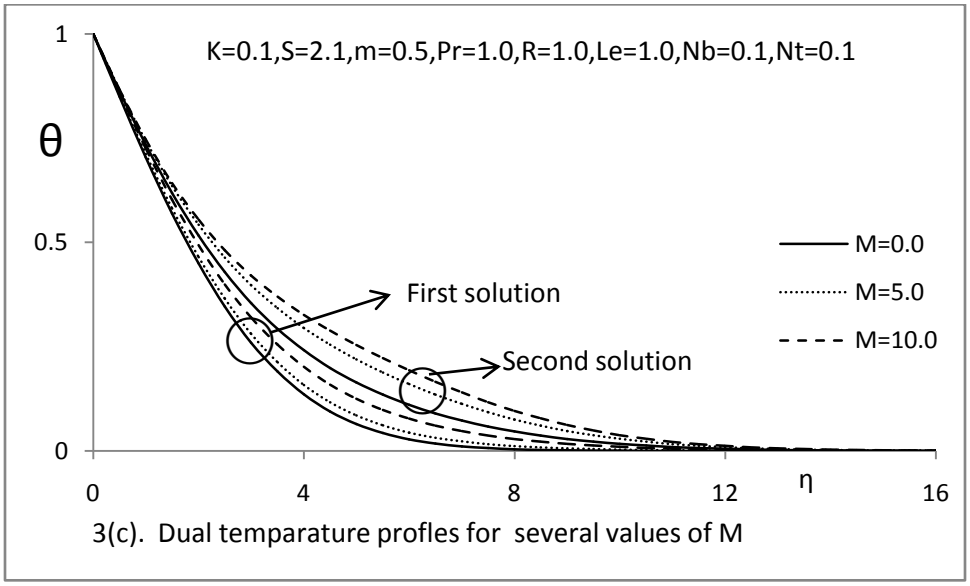

3(c). Dual temparature profles for several values of M

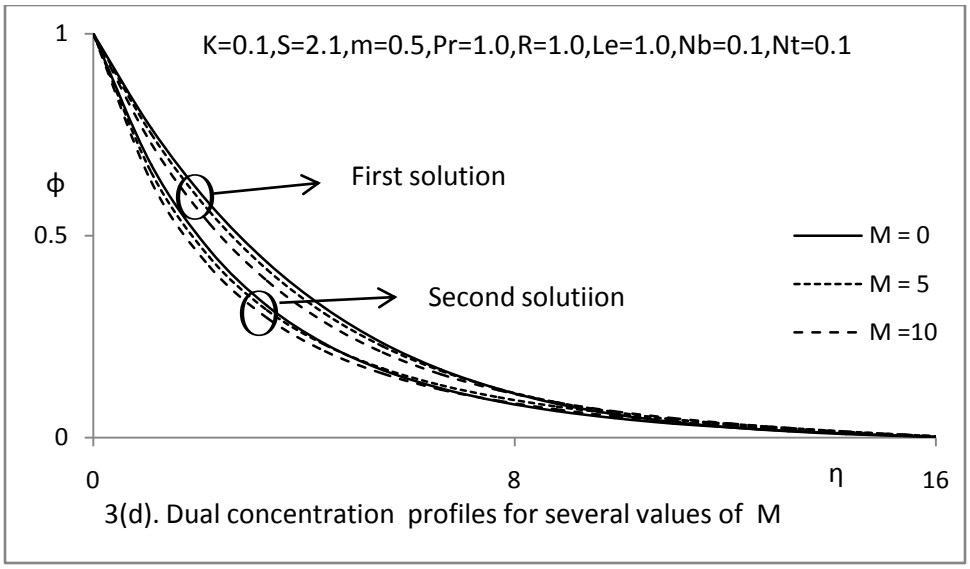

3(d). Dual concentration profiles for several values of M

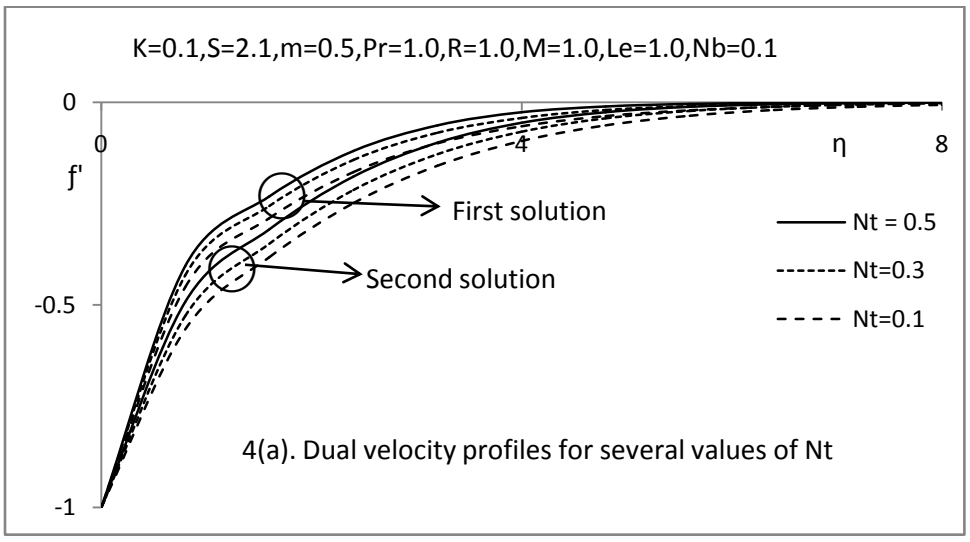

4(a). Dual velocity profiles for several values of Nt

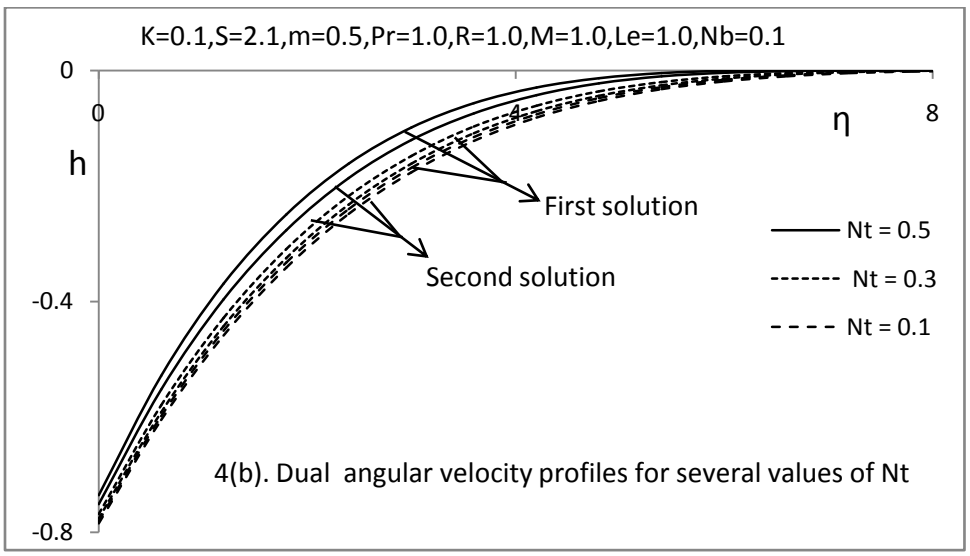

4(b). Dual angular velocity profiles for several values of Nt

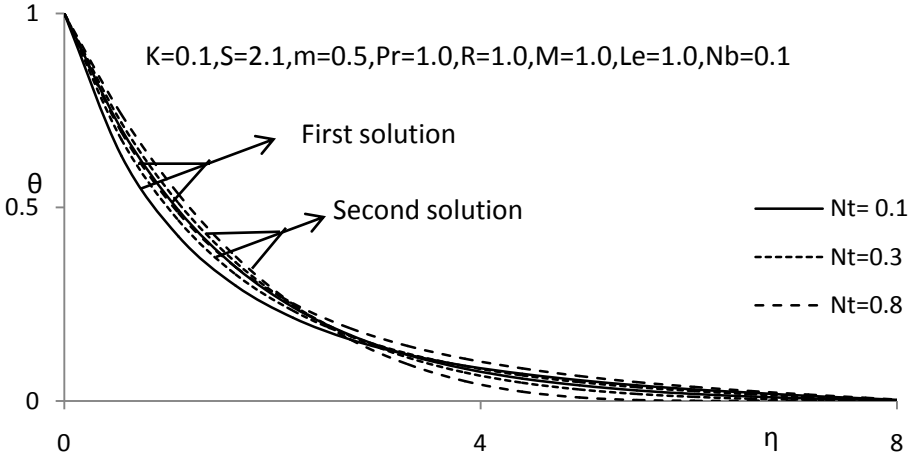

4(c). Dual temparature profiles for several values of Nt

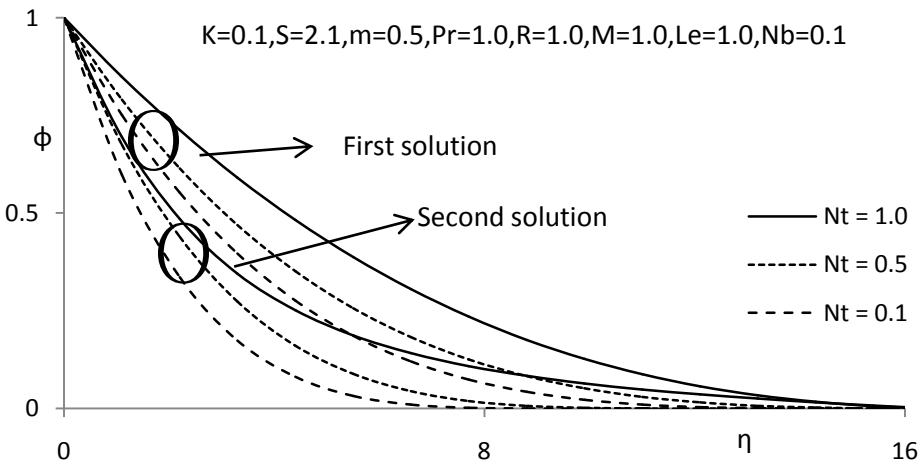

4(d). Dual concentration profiles for several values of Nt

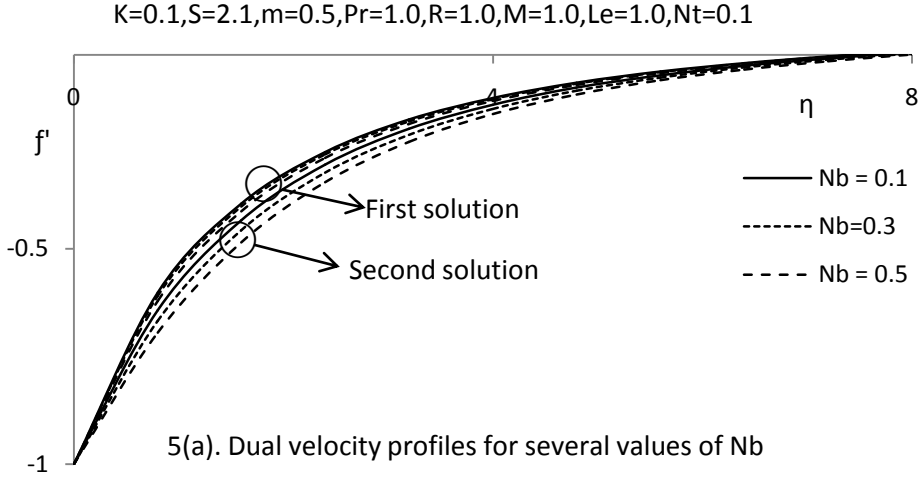

5(a). Dual velocity profiles for several values of Nb

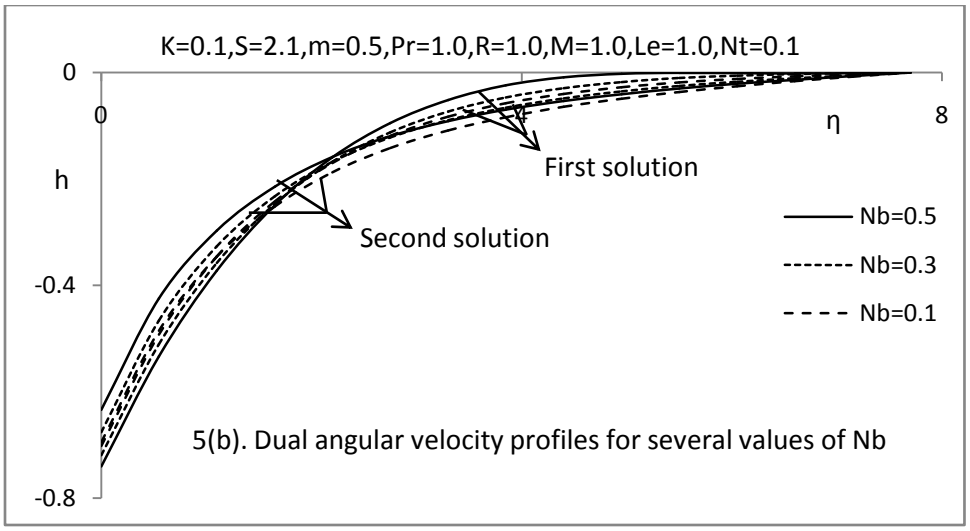

5(b). Dual angular velocity profiles for several values of Nb

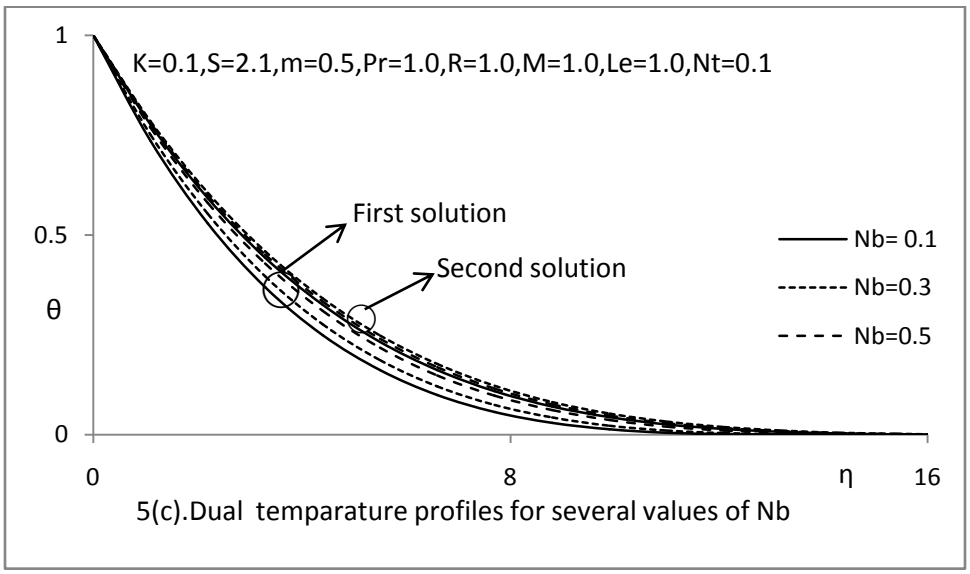

5(c).Dual temparature profiles for several values of Nb

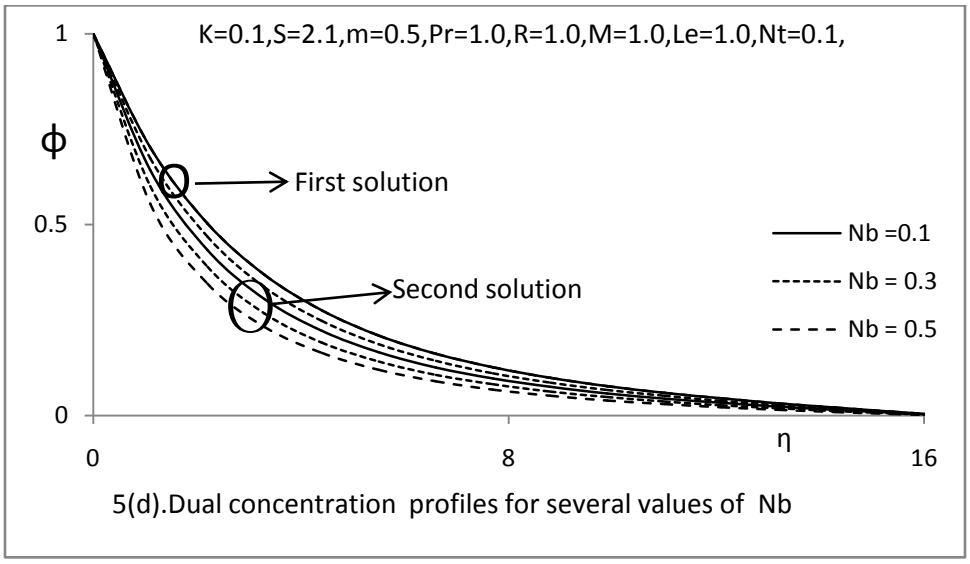

5(d).Dual concentration profiles for several values of Nb

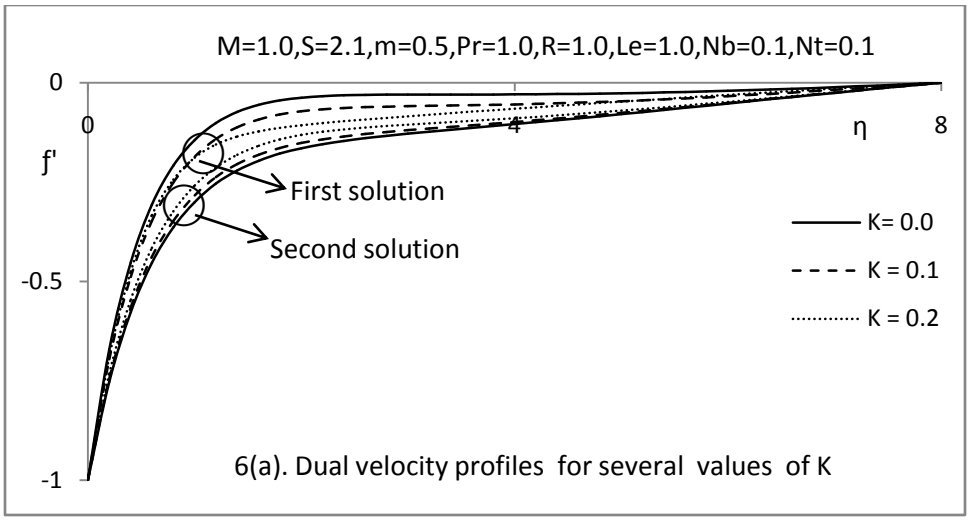

6(a). Dual velocity profiles for several values of K

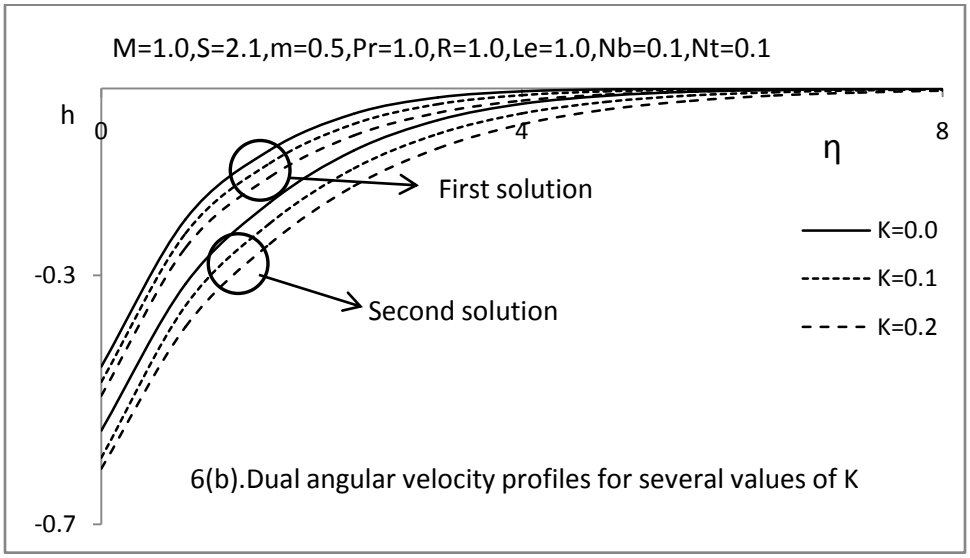

6(b).Dual angular velocity profiles for several values of K

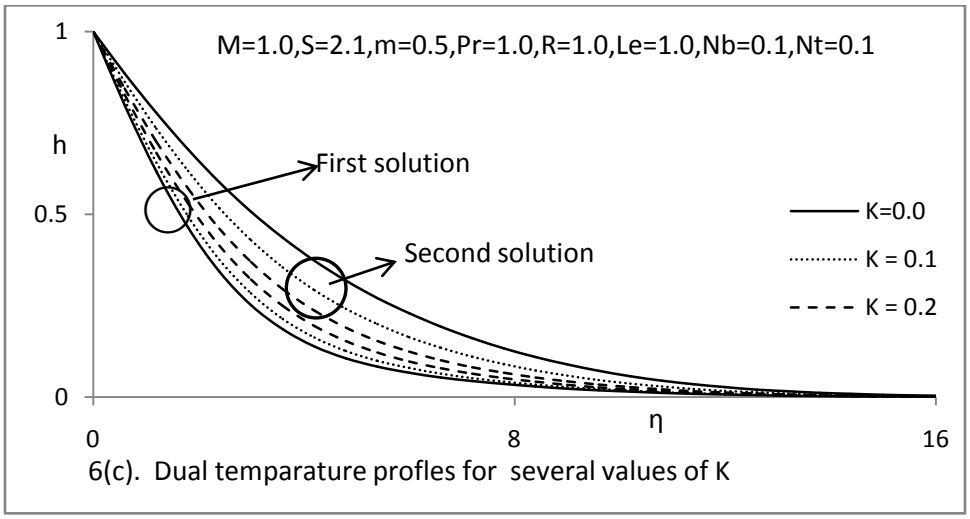

6(c). Dual temparature profles for several values of K

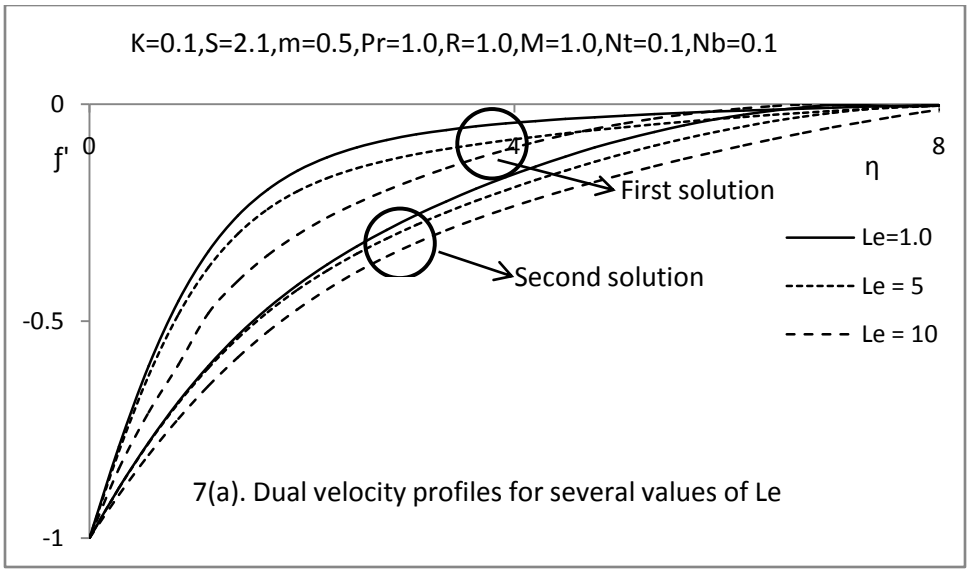

7(a). Dual velocity profiles for several values of Le

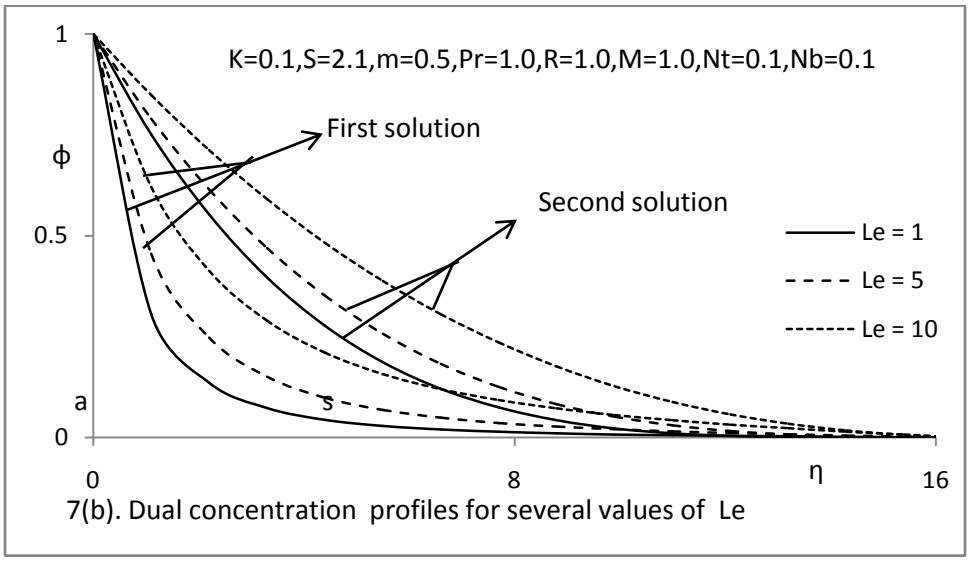

7(b). Dual concentration profiles for several values of Le

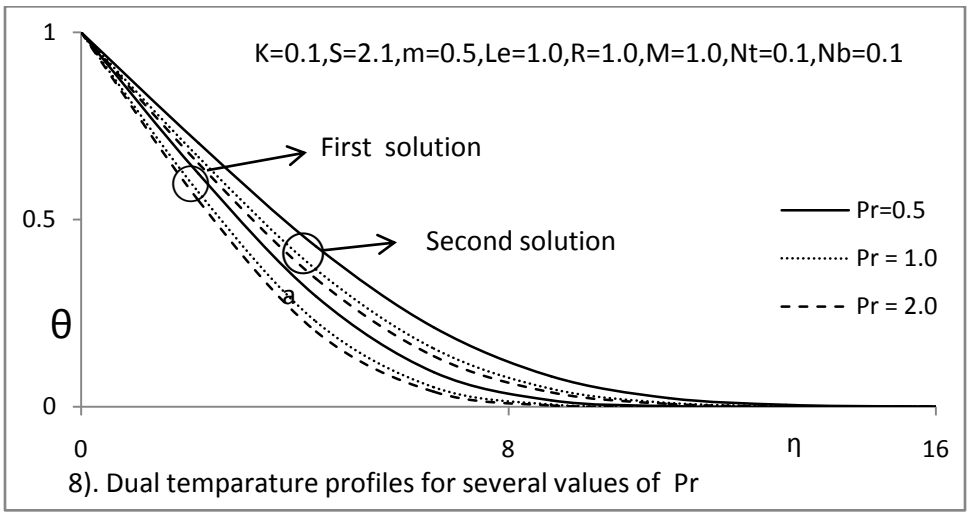

8). Dual temparature profiles for several values of Pr

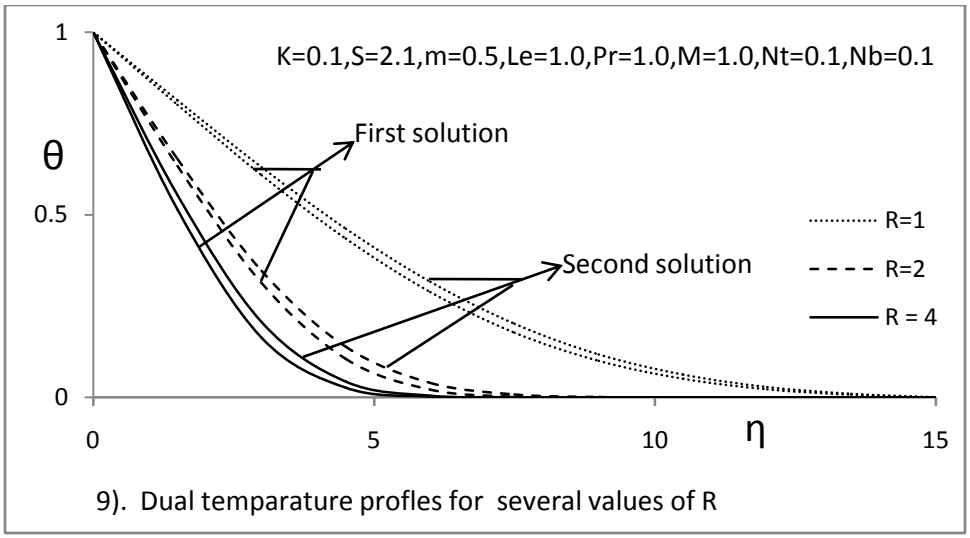

9). Dual temparature profles for several values of R

3. References:

[1] A.C. Eringen, Theory of micropolar fluids, J. Math. Mech. 16 (1966) 1–18.
[2] Eringen AC. Theory of thermomicrofluids. J Math Anal Appl1972;38:480–96.
[3] Ariman T, Turk MA, Sylvester ND. Microcontinuum fluidmechanics: a review. Int J Eng Sci 1973;11:905–30.
[4] Ariman T, Turk MA, Sylvester ND. Microcontinuum fluidmechanics: a review. Int J Eng Sci 1974;12:273–93.
[5] Lukaszewicz G. Micropolar fluids: theory and application. Basel:Birkhauser; 1999.
[6] Eringen AC. Microcontinum field theory II: Fluent media. NewYork: Springer; 2001.
[7] J. Peddieson, R.P. McNitt, Boundary-layer theory for a micropolar fluid, Recent Adv. Eng.Sci.5 (1970) 405–426.
[8] J.Peddieson, An application of the micropolar fluid model to the calculation of turbulent shear flow, Int. J. Eng. Sci. 10 (1972) 23–32.
[9] G. Ahmadi, Self-similar solution of incompressible micropolar boundary layer flow over a semi-infinite plate, Int. J. Eng. Sci. 14 (1976) 639–646.
[10] H. Kummerer, Similar laminar boundary layers in incompressible micropolar fluids, Rheol. Acta 16 (1977) 261–265.
[11] BS Malga, N Kishan ," Viscous Dissipation Effects on Unsteady free Convection and Mass Transfer Flow of Micropolar Fluid Embedded in a Porous Media with Chemical Reaction" Elixir Appl. Math. 63 (2013) 18569-18578.
[12] G.S. Guram, A.C. Smith, Stagnation flow of micropolar fluids with strong and weak interactions, Comput. Math. Appl. 6 (1980) 213–233.
[13] S.K. Jena, M.N. Mathur, Similarity solutions for laminar free convection flow of a thermomicropolar fluid past a non-isothermal vertical flat plate, Int. J. Eng.Sci. 19 (1981) 1431–1439.
[14] R.S.R. Gorla, Micropolar boundary layer flow at a stagnation on a moving wall,Int. J. Eng. Sci. 21(1983)25–33.
[15] Miklavc˘ic˘ M, Wang CY (2006) Viscous flow due to a shrinking sheet. Quart.Appl. Math. 64: 283–290.
[16] Goldstein J (1965) On backward boundary layers and flow in converging passages. J. Fluid Mech. 21: 33–45.
[17] M. Miklavc˘ic˘, C.Y. Wang, Viscous flow due a shrinking sheet, Q. Appl. Math. 64(2006) 283–290.
[18] C.Y. Wang, Liquid film on an unsteady stretching sheet, Q. Appl. Math. 48(1990) 601–610.
[19] T. Fang, Boundary layer flow over a shrinking sheet with power-law velocity,Int. J. Heat Mass Transfer 51 (2008) 5838–5843.
[20] T. Fang, J. Zhang, Closed-form exact solution of MHD viscous flow over a shrinking sheet, Commun. Nonlinear Sci. Numer. Simul. 14 (2009) 2853–2857.
[21] T. Fang, J. Zhang, S. Yao, Viscous flow over an unsteady shrinking sheet with mass transfer, Chin. Phys. Lett. 26 (2009) 014703.
[22] K. Bhattacharyya, Boundary layer flow and heat transfer over an exponentially shrinking sheet, Chin. Phys. Lett. 28 (2011) 074701.
[23] A. Ishak, Y.Y. Lok, I. Pop, Non-Newtonian power-law fluid flow past a shrinking sheet with suction, Chem. Eng. Commun. 199 (2012) 142–150.
[24] N.A. Yacob, A. Ishak, Micropolar fluid flow over a shrinking sheet, Meccanica 47 (2012) 293–299.
[25] C.Y. Wang, Stagnation flow towards a shrinking sheet, Int. J. Non-Linear Mech. 43 (2008) 377–382.
[26] E.M.A.Elbashbeshy, Radiation effect on heat transfer over a stretching surface, Can. J.Phys.78 (2000) 1107–1112.
[27] K. Bhattacharyya, S. Mukhopadhyay, G.C. Layek, Slip effects on boundary layer stagnation-point flow and heat transfer towards a shrinking sheet, Int. J. Heat Mass Transfer 54 (2011) 308–313.
[28] Choi SUS (1995) Enhancing thermal conductivity of fluids with nanoparticles, Developments and Applications of Non-Newtonian Flows. FED-vol.231/MDvol. 66: 99–105.
[29]. Li Y, Zhou J, Tung S, Schneider E, Xi S (2009) A review on development of nanofluid preparation and characterization. Powder Tech. 196: 89–101.
[30]. Kakac¸ S, Pramuanjaroenkij A (2009) Review of convective heat transfer enhancement with nanofluids. Int. J. Heat Mass Transfer 52: 3187–3196.
[31]. N. Kishan and D Hunegnaw, "MHD Boundary Layer Flow and Heat Transfer Over a Non-Linearly Permeable Stretching/Shrinking Sheet in a Nanofluid with Suction Effect, Thermal Radiation and Chemical Reaction." *Journal of Nanofluids*", volume.3, pages1-9. 2014.
[32]. Wong KV, De Leon O (2010) Applications of nanofluids: current and future. Adv. Mech. Eng. 2010: Article ID 519659, 11 pages.
[33]. Saidur R, Leong KY, Mohammad HA (2011) A review on applications and challenges of nanofluids. Renew. Sust. Ener. Rev. 15: 1646–1668.
[34]. Mahian O, Kianifar A, Kalogirou SA, Pop I, Wongwises S (2013) A review of the applications of nanofluids in solar energy. Int. J. Heat Mass Transfer 57: 582–594.

[35]. Khanafer K, Vafai K, Lightstone M (2003) Buoyancy-driven heat transfer enhancement in a two-dimensional enclosure utilizing nanofluids. Int. J. Heat Mass Transfer 46: 3639–3653.
[36]. Tiwari RK, Das MK (2007) Heat transfer augmentation in a two-sided liddriven differentially heated square cavity utilizing nanofluids. Int. J. Heat Mass Transfer 50: 2002–2018.
[37]. Buongiorno J (2006) Convective transport in nanofluids. ASME J. Heat Transfer 128: 240–250.
[38]. Nield DA, Kuznetsov AV (2009) The Cheng-Minkowycz problem for natural convective boundary layer flow in a porous medium saturated by a nanofluid. Int. J. Heat Mass Transfer 52: 5792–5795.
[39]. Kuznetsov AV, Nield DA (2010) Natural convective boundary-layer flow of a nanofluid past a vertical plate. Int. J. Therm. Sci. 49: 243–247.
[40] Srinivas Maripala and Kishan.N," Unsteady MHD flow and heat transfer of nanofluid over a permeable shrinking sheet with thermal radiation and chemical reaction", American Journal of Engineering Research (AJER) Volume-4, Issue-6, pp-68-79(2015).
[41]. Krishnendu Bhattacharyya, Swati Mukhopadhyay, G.C.Layek, studied the "Effects of thermal radiation on micropolar fluid flow and heat transfer over a porous shrinking sheet". International Journal of Heat and Mass Transfer 55(2012) 2945-2952.
[42]S.K. Jena, M.N. Mathur, Similarity solutions for laminar free convection flow of a thermomicropolar fluid past a non-isothermal vertical flat plate, Int. J. Eng. Sci. 19 (1981) 1431–1439.
[43] G.S. Guram, A.C. Smith, Stagnation flow of micropolar fluids with strong and weak interactions, Comput. Math. Appl. 6 (1980) 213–233.
[44]G. Ahmadi, Self-similar solution of incompressible micropolar boundary layer flow over a semi-infinite plate, Int. J. Eng. Sci. 14 (1976) 639–646.
[45] J. Peddieson, An application of the micropolar fluid model to the calculation of turbulent shear flow, Int. J. Eng. Sci. 10 (1972) 23–32.
[46] R.S.R.Gorla, Micropolar boundary layer flow at astagnation on a moving wall, Int. J. Eng.Sci. 21 (1983) 25–33.
[47]A. Ishak, R. Nazar, I. Pop, Heat transfer over a stretching surface with variable heat flux in micropolar fluids, Phys. Lett. A 372 (2008) 559–561.
[48] M.Q. Brewster, Thermal Radiative Transfer Properties, John Wiley and Sons,1972